Pak. J. Bot., 47(4): 1459-1465, 2015.

CYTOLOGICAL OBSERVATION OF *SOLANUM PIMPINELLIFOLIUM* L. MICROSPORE DEVELOPMENT

HAIOU QU[1,2], JANARTHINI SEBASTIAN RYLOSONA[1] AND LINGXIA ZHAO[1,2*]

[1] Joint Tomato Research Institute, School of Agriculture and Biology, Shanghai Jiao Tong University, Shanghai 200240, China; [2]Plant Biotechnology Research Center, Shanghai Jiao Tong University, Shanghai 200240, China
[*]Corresponding author: e-mail: lxzhao@sjtu.edu.cn; Phone: 86-21-34205775; Fax: 86-21-34205775

Abstract

Tomato (*Solanum lycopersicum* L.) is one of the most important horticultural crops worldwide, and has also been adapted as a model plant in a wide range of research disciplines. However, stamen development in tomato is less known than other model species, such as *Arabidopsis thaliana* and *Oryza sativa* L. (rice). In order to understand tomato flower development in more detail, the key goal of this study was to establish a precise correlation between visual morphological features and cytological events. To this end, we characterized a wild tomato species, *S. pimpinellifolium* (accession LA1585), to define stamen developmental stages using semi-thin sectioning. Based on distinct stages of flower development, *S. pimpinellifolium* anther/stamen development was divided into ten stages, and characteristic morphological and cytological features in stamens at each developmental stage were identified. In this way, flower characteristics and microspore development were correlated. In addition, specific cytological key events in *S. pimpinellifolium* were compared with those in *A. thaliana* and rice at corresponding stages, as well as with those in domesticated tomato (*S. lycopersicum* L.), and the differences are discussed.

Key words: *Solanum pimpinellifolium*, Cytological observation, Tomato

Introduction

In angiosperms, microsporogenesis occurs within the anther, which has a four-lobed structure (Goldberg *et al*., 1993), and microspore cell-specification and differentiation events within the anther gives rise to mature pollen grains that contribute to male reproductive success. The formation of microspores, which develop into the male gametophyte in land plants, has been studied in detail in a number of model species, including *Arabidopsis thaliana* (Sanders *et al*., 1999), *Zea mays* (Barnabas *et al*., 1987), *Oryza sativa* (Zhang & Wilson, 2009; Zhang *et al*., 2011) and *Nicotiana tabacum* (Koltunow *et al*., 1990), as well as Ginkgo biloba (Sun *et al.*, 2015) and family Lamiaceae (Firdous *et al.*, 2015), and a defined set of developmental stages over a specific timescale have been reported for these model species. However, this is not the case for many horticulturally valuable species, even though microspore development is critical for fruit set, and so underlies fruit development and yield.

Tomato (*S. lycopersicum*) is one of the most economically important horticultural crops, with an estimated 159 billion tons in global annual yield from 4.73 million hectares, which is preceded only by potato as the most consumed vegetable crop from the Solanaceae or Nightshade family (http://www.fao.org/corp/statistics/en). Tomato has also emerged as a model plant for experimental biologists working in a wide range of research disciplines, including genetics (Chetelat & Meglic, 2000; Tanksley, 2004), evolution (Peralta *et al*., 2006; Moyle, 2008), reproductive biology (Li & Chetelat, 2010; Bedinger *et al*., 2011) and genome-scale analyses (Alba *et al*., 2005; Mueller *et al*., 2005; Yeats *et al*., 2010; Matas *et al*., 2011; Osorio *et al*., 2011; Sato *et al*., 2011). Despite its importance, the literature regarding tomato microsporogenesis is sparse compared to the monocotyledonous rice (Poaceae family) and the dicotyledonous *A. thaliana* (Cruciferae family) (Sawhney & Bhadula, 1988; Sanders *et al*., 1999; Zhang & Wilson, 2009), and it is not known whether there are differences in microspore development between tomato and the better studied model species.

The development of tomato microspores has previously been divided into eight stages based on bud length (Sawhney & Bhadula, 1988), and detailed studies of pollen development have revealed ultrastructural differences from the tetrad stage to pollen maturation (Polowick & Sawhney, 1992; 1993a; 1993b), as well as the developmental transition of microspores and flowers in wild type tomato genotypes and tomato mutants (Sawhney & Bhadula, 1988; Polowick & Sawhney, 1995; Brukhin *et al*., 2003). However, to our knowledge, microspore development has only been studied in domesticated tomato (*S. lycopersicum*) or *S. lycopersicum* var. cerasiforme, which has only a few flowers on each inflorescence (Polowick & Sawhney, 1993b; Brukhin *et al*., 2003). Consequently, within the genus *Solanum*, correlations between morphological features of the visible buds/flowers and microspore development over a defined time scale are not well defined, unlike the situation for rice and *A. thaliana* (Ma, 2005; Zhang *et al*., 2011; Chang *et al*., 2011;Yousuf *et al*., 2006).

In this regard, in order to effectively characterize the chemical, physiological and structural differences as well as the regulation and expression of stamen development associated genes, it is important to establish a precise correlation between the morphological features and key cytological events at each developmental stage (Yousuf *et al*., 2009). In the present study, we characterized microspore development at different developmental stages in wild tomato relative, *S. pimpinellifolium* (LA1585), since this species has ten or more buds/flowers in each inflorescence before anthesis, which allows the accurate staging of microspore development over a well-defined time scale. In addition to being the wild relative that is most closely related to cultivated tomato, *S. pimpinellifolium* can also

cross freely with the domesticated species (Miller & Tanksley, 1990; Alvarez *et al*., 2001; Marshall *et al*., 2001), and it has the important characteristic that anthesis can occur over the entire year. In this study, changes in *S. pimpinellifolium* cytology during microspore development were observed in semi-thin sections and key features of *S. pimpinellifolium* microspore development were compared with those of the two experimental model plants, *A. thaliana* and rice, as well as with the equivalent features in *S. lycopersicum*.

Materials and Methods

Sample collection: Seeds of *S. pimpinellifolium* (accession LA1585) were kindly provided by the Tomato Genetic Resource Center (TGRC, http://tgrc.ucdavis.edu), and sown on petri dishes with 1/2 MS medium (Murashige and Skoog, MS basal medium 2.21 g/L, sucrose 20 g/L, phytogel 2.6 g/L, Sigma, pH 5.8). The plates were then incubated at 25°C, with a photoperiod of 16h light /8h dark to promote germination and seedlings were then transferred to sterile plastic pots (diameter 7.5 cm) containing seedling soil (20% vermiculite , 20% turf soil and 60% garden soil) and allowed to grow until four true leaves had fully spread. The plantlets were then transferred into 5 L plastic pots with nutrient soil (50% peat, 20% vermiculite and 30% soil) and grown in a greenhouse (25°C day/18°C night, 70% air humidity and natural light) in the School of Agriculture and Biology, Shanghai Jiao Tong University, China.

Inflorescences and flowers were sampled from healthy blossoming plants where only one open flower and small buds (generally more than ten) were present. Harvested inflorescences and flowers were brought back to the laboratory in an ice box. Photographs of the different developmental stages were taken with a digital camera (SONY Cyber-shot DSC-W350, Japan).

Histological analysis: The anthers or intact small buds at different development stages were harvested from the selected inflorescences using sterile forceps before being fixed in FAA (50% ethanol, 5.0% glacial acetic acid, 3.7% formaldehyde) overnight, and subsequently dehydrated in a graded ethanol series (2×50%, 60%, 70%, 85%, 95%, 3×100%) for 30 min. Sample were then embedded in Technovit 7100 resin (Emgrid Australia Pty Ltd, Australia), and sectioned (2 μm) using a microtome (Leica RM2265, Germany). Transverse sections of anthers derived from different development stages were stainedwith 1% toluidine blue for 20 s and observed under a microscope (Olympus BX51, Japan).

Results

Flower features: *S. pimpinellifolium* (accession LA1585) is a small perennial bush with a slim stem and a uniparous scorpioid cyme, with more than ten flowers per inflorescence (Fig. 1A). Generally, a perfect flower consists of five sepals, alternating with five petals and a style surrounded by stamens, where five anthers are connection laterally to form a flask-shaped cone with an elongated sterile tip at the apex (Fig. 1A and B). The long style, which projects from the anther cone in *S. pimpinellifolium* at anthesis, is distinct from that of the cultivated tomato which is embedded within the anther cone (Fig. 1A and C). Ten buds/flower, including one open flower and nine buds, which harvested from same inflorescence and ranged from 3.5 mm to 11.5 mm in length, and these were divided into ten stages of anther development (Fig. 1C). Landmark cytological events for each *S. pimpinellifolium* stamen developmental stage were noted over a time course starting from the emergence of the U-shaped sporogenous cell region to the release of mature pollen from the anther locules (Fig. 2 and Fig. 3).

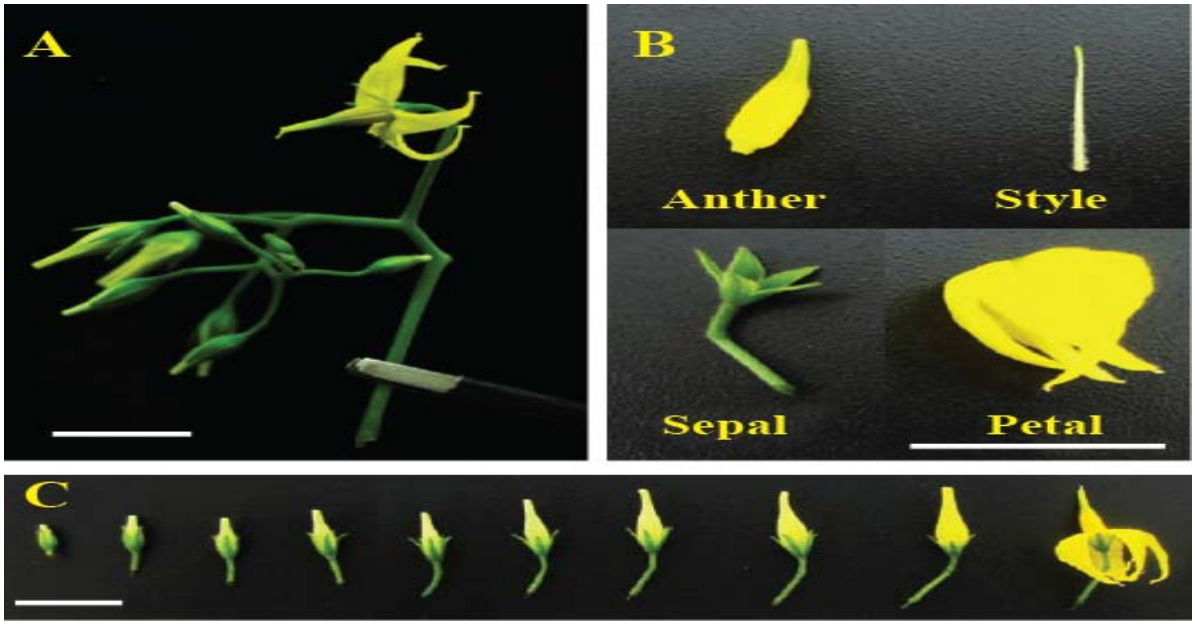

Fig. 1. Buds/flowers and inflorescence of *Solanum pimpinellifolium*.
A: a scorpioid cyme inflorescence; **B**: a perfect flower with sepal, petal, anther and carpel; **C**: developing buds/flower from stages 1 to 10. (Bars=10mm).

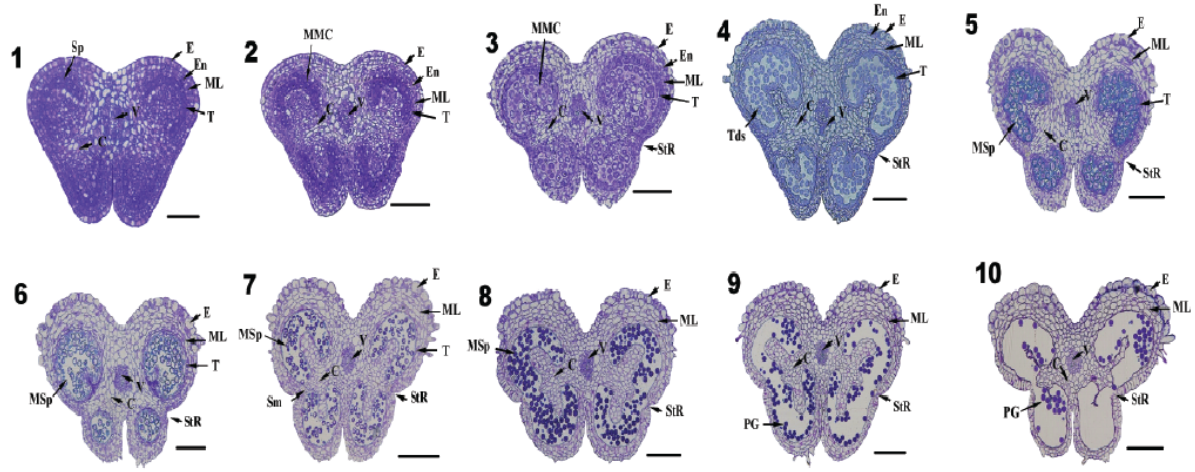

Fig. 2. *Solanum pimpinellifolium* anther development
Arabic numerals 1 to 10 indicate anther development stages. Flowers were fixed and embedded in LR-White plastic resin and sectioned into 2 mm transverse sections. The flower sections were stained with toluidine blue and anthers were imaged with a bright-field microscopy. ***BM***, binucleate microspore; *C*, connective tissue; ***E***, epidermis; ***En***, endothecium; ***ML***, middle layer; ***MMC***, microspore mother cells; ***MSp***, microspores; ***PG***, pollen grains; ***Sm***, septum; ***Sp***, sporogenous cells; ***St***, stomium; ***StR***, stomium region; ***T***, tapetum; ***Tds***, tetrads; ***V***, vascular bundle; ***Va***, vacuoles (bars, 1 to 6 =100 µm; 7 to 10= 200 µm).

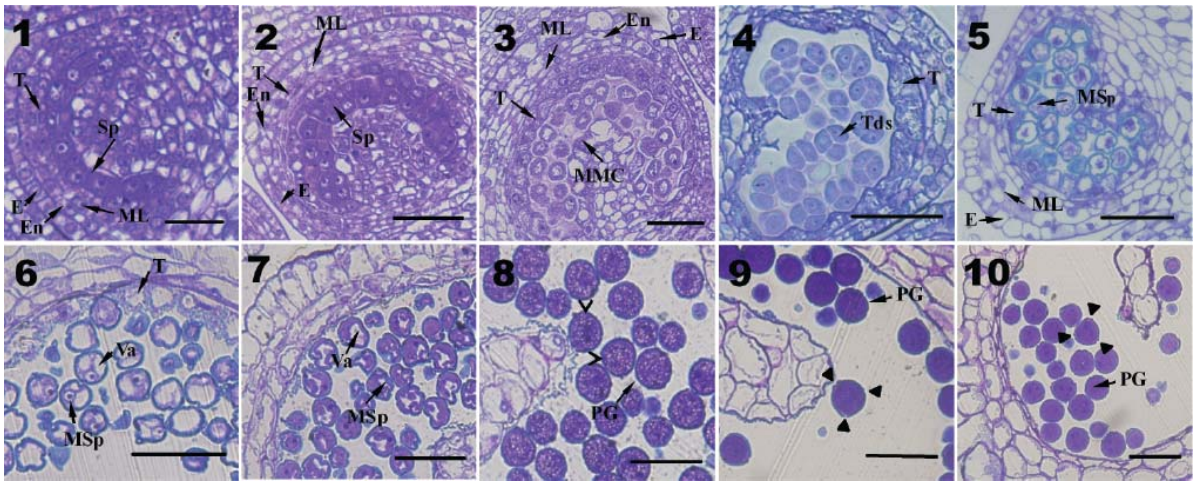

Fig. 3. Magnification of *Solanum pimpinellifolium* anther development
Arabic numerals 1 to 10 represent anther developmental stages. ***BM***, binucleate microspore; ***C***, connective tissue; ***E***, epidermis; ***En***, endothecium; ***ML***, middle layer; ***MMC***, microspore mother cells; ***MSp***, microspores; ***PG***, pollen grains; ***Sm***, septum; ***Sp***, sporogenous cells; ***St***, stomium; ***StR***, stomium region; ***T***, tapetum; ***Tds***, tetrads; ***V***, vascular bundle; ***Va***, vacuoles (bars=50 µm). **Arrowhead** indicates vegetative and generative nucleus; **solid triangle** indicates germinal apertures.

Stage 1; the early sporogenesis stage: At stage 1, the bud length was approximately 3.5 mm, and a yellow colored corolla showed the first signs of emergence from the enwrapping sepals (Fig. 1C). The fully developed anther was divided into a bilateral structure (two half anthers) with an anther wall, connective tissue, vasculature and four locule regions. Each anther half included two separate locules (the outer being larger than the inner), and each locule region was filled by two layers of sporogenous cells (Sp) and the clevis, or U-shaped locule region was surrounded by the tapetum (Fig. 2A). The anther wall differentiated into four distinct cellular layers: an epidermis layer (E), an endothecium layer (En), a middle layer (Ml) and a tapetum layer (T), each comprising a single layer of cells (Fig. 2, stage 1; Fig. 3, stage 1).

Stage 2; the late sporogenesis stage: At stage 2, bud lengths reached 4.5 mm, the corollaceous top was distinctly exposed from the calyx, and sepals initiated opening (Fig. 1C). The distinct E, En, Ml and T cell layers in the anther showed continued development and cell number gradually increased in both the E and En layers due to periclinal division and the cell number of the Ml cell layer also increased, giving rise to three or four layers due to anticlinal division. The 'U'-shaped Sp cells initiated differentiation into microspore mother cells (MMC), and those MMCs were stained with toluidine blue to reveal a distinct blue-black region. At this stage, the tapetum cell layer was thicker and intact (Fig. 2, stage 2; Fig. 3, stage 2).

Stage 3; the MMC formation stage: At stage 3, sepals were only half the length of the corolla (Fig. 1 C). The MMCs showed evidence of vacuolation, with an enlarged locular space and they also entered meiosis. A concave stomium region (Str) arose at both sides of the anther, the outer tapetum layer became gradually thicker and the emergence of binucleate tapetum cells was the most notable characteristic of this stage. The outer E cells increased in size and were observed to be larger than the inner E cells (Fig. 2, stage 3; Fig. 3, stage 3).

Stage 4; the tetrad stage: At stage 4, all flower organs continued developing and some sepals expanded further (Fig. 1C). The MMCs underwent one round of meiosis and mitosis and differentiated into tetrads that were coated by callose. Concomitantly, the cells of the tapetum layer, which supply nutrients to the developing microspores, began to burst and form an amoeboid shape, in contrast to the previous uniform appearance of the cells in the tapetum layer (Fig. 2, stage 4; Fig. 3, stage 4).

Stage 5; the early uninucleate microspore stage: At stage 5, all sepals were fully open (Fig. 1C). Free haploid microspores (Msp) were released from the irregularly shaped callose enwrapped tetrads in each of the four locules, the nucleolus was densely stained by toluidine blue and most of the Msps had a larger vacuole. The tapetal layer showed evidence of continued degeneration (Fig. 2, stage 5; Fig. 3, stage 5).

Stage 6; the late uninucleate microspore stage: At stage 6, buds reached approximately 8.5 mm in length, and the lower part of the corolla began to swell as the anther surrounded by petals developed quickly (Fig. 1C). Microspores were converting from their irregular shape into angular structures, and the blue-black toluidine blue staining associated with the nucleus was localized in the limbic regions of the microspores. The cells of the tapetum layer degenerated further and only some patches remained (Fig. 2, stage 6; Fig. 3, stage 6).

Stage 7; the vacuolated microspore stage: At stage 7, the sepals only reached one-third of the length of the corolla, and the lower part of the corolla expanded further (Fig. 1C). The angular microspores adopted a more spherical shape and both more extensive vacuolation and a high density of nuclear substances were observed in the microspores. Although remnants of a very thin tapetum layer were still be detected, the septum layer became considerably thinner and only a remnant wall of broken tapetum cells remained. Septum (Sp) tissues, which were located between the two locules in each half of the anther, began to disappear due to cell degradation (Fig. 2, stage 7; Fig. 3, stage 7).

Stage 8; the binucleate microspore stage: At stage 8, buds were 10.5 mm in length and the corolla size increased to become equal to that of an open flower, while the top of the corolla was still closed (Fig. 1C). The large vacuole within the microspores disappeared, or was converted into many smaller vacuoles, and the irregularly shaped microspores were present as spherical binucleate pollen grains (PGs), which stained blue-black with toluidine blue. The tapetum layer had entirely disappeared from the locules and the cells of the Sp were completely absorbed or degraded, resulting in an opening between the locules. The two locules started to form one larger locule in each half of the anther, and the PGs were able to freely move within this larger locule. Eventually, anthers with four locules converted into anthers with two larger locules. Meanwhile, the cells of the stomium (St) also started to degenerate and form a thin layer of only one or two cell layers (Fig. 2, stage 8; Fig. 3 stage 8).

Stage 9; the early mature pollen stage: At stage 9, the buds were approximately 11.0 mm in length, and the flat top of the yellow corolla had opened appreciably (Fig. 1C). The smaller vacuoles within the pollen grains disappeared, and mature pollen grains, which stained very strongly blue-black with toluidine blue, were present. Three distinct colporates/germinal apertures were observed on each of the spherical pollen grains. Stomium cells were gradually absorbed and only one or two layers cells remained, but the anther sporangium was intact (Fig. 2, stage 9 and Fig. 3, stage 9).

Stage 10; the late mature pollen stage: At stage 10, the corolla had opened fully and the bright-yellow petals curled down in the direction of the peduncle, exposing the bright-yellow anther cone and the style projecting from the anther cone (Fig. 1C). Finally, the anther sporangium dehisced due to degeneration of the stomium cells, and mature pollen grains were released from the locules, where only a few pollen grains remained (Fig. 2, stage 10; Fig. 3, stage 10).

Discussion

Microspore development in angiosperms starts with the formation a stamen primordium and ends with the maturation of the pollen grains and this process has been characterized and staged in a number of model species (Sanders *et al*., 1999; Brukhin *et al*., 2003; Zhang & Wilson, 2009). Tomato has emerged as a model plant for researchers in a wide range of research disciplines (Li & Chetelat, 2010; Yeats *et al*., 2010; Bedinger *et al*., 2011; Matas *et al*., 2011), and the precise definition of microspore developmental stages is therefore essential for studies of tomato reproductive and developmental biology. In this current study, the wild tomato species, *S. pimpinellifolium* (LA1585), was chosen for a detailed study of microspore development stages, since it is taxonomically placed between domesticated tomato and other wild relatives, with the closest relationship being to domesticated tomato (Zuriaga *et al*., 2009). To our knowledge, domesticated tomato has to date served as the primary experimental material for the analysis of tomato microspore development (Mazzucato *et al*., 1998; Sawhney & Bhadula 1998; Brukhin *et al*., 2003); however, domesticated tomato differs from *S. pimpinellifolium* in the number of flowers on each inflorescence, where ten or more buds/flower are present in *S. pimpinellifolium*, compared to only a few in *S. lycopersicum*. This characteristic of *S. pimpinellifolium* facilitates a fine dissection of stamen development over a time course.

Table 1. Major events during tomato anther development compared with *A. thaliana* and rice [a].

Tomato anther stage	Tomato anther length (mm)	*A. thaliana* anther stage[b]	Rice anther stage[c]	Major events and morphological markers	Tissues present
1	~2.63	3 ~ 4	3~4	Emergence of the U-shaped sporogenous cell region and formation of the four-lobed anther pattern. The vascular region was clearly visible.	E, En, Ml, V, T , C, Sp
2	2.64~3.33	4~5	5~6	The number of MMCs increased due to anticlinal division; the middle layer also increased but due to periclinal division.	E, En, Ml, V, T, C, MMC
3	3.34~3.81	6	6~8a	MMCs initiated genomic DNA replication, and entered meiosis and mitosis. The tapetum layer became thicker, and the size and number of tapetum cells increased due to anticlinal division and growth, and generated binucleate tapetum cells. Stomium regions emerged between two locules in each anther half and the middle layer initiated degradation.	E, En, Ml, V, T , C, MMC, StR
4	3.82~4.19	7	8b	MMCs completed meiosis and generated free microspore tetrads within each locule. Only one thin layer of the middle layer was present. The tapetum layer started to degrade.	E, En, Ml, V, T , C, StR, Tds
5	4.20~4.58	8	9~10	Individual microspores, surrounded by a callose cell wall, were released from the tetrads, and vacuolated into irregular shapes, and underwent one round of mitosis. The tapetum layer became thinner due to the degradation of cells and only one of layer cells remained as the middle layer.	E, En, V, T , C, StR, Msp
6	4.59~5.32	8	10	Microspores were further vacuolated and generated three-celled microspores. The tapetum degraded further. The shapes were similar to those seen in *A. thaliana* but not rice.	E, En, V, T , C, StR, Msp
7	5.33~6.66	9~10	11~12	Microspores generated an exine wall, and changed from an irregular to a spherical shape. Septum tissue became thin. Stomium tissue differentiation began and only a few remnants of the tapetum remained.	E, En, V, T , C, StR, Msp
8	6.67~7.93	12	13	The microspore exine walls generated numerous granules that resulted in a rough surface on the pollen grains. Septum cells fully degraded resulting in an opening between the two locules in each anther half. Stomium cells continued to degrade.	E, En, V, C, StR, Mp
9	7.94~8.72	12	13	Three colporates/germinal apertures were presented on the surface of the pollen grains. Only one layer of cells remained in the stomium.	E, En, V, C, StR, Mp
10	8.73~9.06	13~14	13~14	Stomium cells were fully degraded and a cleft emerged on the outside of each anther half. Mature pollen grains were released from the anthers.	E, En, V, C, Mp

[a] ***BM***, binucleate microspore; ***E***, epidermis; ***En***, endothecium; ***ML***, middle layer; ***MMC***, microspore mother cells; ***MSp***, microspores; ***PG***, pollen grains; ***Sm***, septum; ***Sp***, sporogenous cells; ***St***, stomium; ***StR***, stomium region; ***T***, tapetum; ***Tds***, tetrads; ***V***, vascular bundle; ***Va***, vacuoles

[b,c] The *A. thaliana* and rice data in the table are based on Sanders *et al.* (1999) and Zhang and Wilson (2009), respectively.

Based on the bud/flower length, which ranged from 3.5 mm to 11.5 mm, or the flower number, the stamen development was divided into ten stages (Fig. 1C). The landmark morphological and cytological events associated with each developmental stage were determined and compared to those of *A. thaliana* and rice at the corresponding stages (Table 1). We propose that the emergence at stages 1 and 2 in *S. pimpinellifolium* of specific sporogenous cells (Sp) and their differentiation into MMCs is equivalent to stages 4 and 5 in both *A. thaliana* and rice (Table 1). The U-shaped region of the Sps and MMCs was only found in tomato since connective tissue projected inward to the locules in the anther, which was not the case in *A. thaliana* and rice (stages 1 and 2 Fig. 2; Sanders *et al*., 1999; Zhang &Wilson, 2009). We also observed two locules in each half of the anther in *S. pimpinellifolium*, which were different in size, with the outer locule (close to the petals) being larger than inner (close to pistil) locule (Fig. 2). This is similar to what is seen in *A. thaliana*, but not in rice (Sanders *et al*., 1999; Zhang &Wilson, 2009).This feature might be related to the specific flower structure in tomato and Arabidopsis that sepals and petals closely pack the anther cone, but it maintains unknown whether extensively existing in dicotyledonous plants. Three colporates/germinal apertures were detected in *S. pimpinellifolium*, but not in *A. thaliana* and rice (stages 8 and 9 in Fig. 2; stages 8 and 9 in Fig. S1; Sanders *et al*., 1999; Zhang & Wilson, 2009). In addition, we also observed that stage of the tapetum layer degradation was different in *S. pimpinellifolium* from what has been reported for *A. thaliana* and rice (Sanders *et al*., 1999; Zhang &Wilson, 2009). Indeed, numerous differences in stamen development were seen between tomato and the two other model species, which presumably lend some evolutionary advantage; however, the adaptive significance of these features remains unknown.

S. lycopersicum flower development, and specifically that of the stamen and carpel, has been divided into twenty stages (Brukhin *et al*., 2003), ranging from the sepal primordial stage (stage 1) to the anther dehiscence stage (stage 19), as well as the stage where the corolla is fully expanded (stage 20) and the pollen and ovules are mature (stage 20). The emergence of MMCs that had differentiated from sporogenous cells (Sp) was observed at stage 1 in *S. pimpinellifolium* and stage 7 in *S. lycopersicum*, while mature pollen release from each of the anther locules occurred at stage 10 in *S. pimpinellifolium* and at stage 20 in *S. lycopersicum* (Fig. 2 and Brukhin *et al*., 2003). We observed that some morphological characteristics of the *S. pimpinellifolium* flower were somewhat different from those of *S. lycopersicum* during stamen development. In *S. lycopersicum*, the calyx emerged at the top of the bud at stage 12, sepals (5.0 mm) were longer than the petals (4.5 mm in length), and free irregularly shaped microspores were released from the tetrads. The corolla protruded from the calyx at stage 13, and the sepals (5.4 mm) were somewhat shorter than the petals (5.8 mm) (Brukhin *et al*., 2003). However, in *S. pimpinellifolium* the corolla emerged from the calyx at stage 1 and, at the same time, stamen development was associated with the differentiation of sporogenous cells (Sp), making this stage equivalent to stage 7 in *S. lycopersicum*. Free, irregularly shaped microspores released from the tetrads were observed at stage 5 in *S. pimpinellifolium* (Fig. 2 stage 5 and Fig. 3 stage 5), where the sepals reached half the length of the petals, while the corolla was still surrounded by sepals in *S. lycopersicum* (Brukhin *et al*., 2003). Initiation of the tapetum layer degeneration occurred at stage 13 in *S. lycopersicum*, a stage where the corolla first emerged from the calyx; however the cells of the *S. pimpinellifolium* tapetum layer began to degenerate at stage 4 (Fig. 2 stage 4), at which time the corolla was already projecting beyond the calyx (Fig. 1C). These results suggest differences between *S. pimpinellifolium* and *S. lycopersicum* in both morphological features and microspore developmental processes during stamen developmental, and that data derived from studies of *S. lycopersicum* are not fully analogous to *S. pimpinellifolium* or other wild tomato species. Consequently, the results derived from *S. pimpinellifolium* might be more applicable for research into the morphology, histology and cytology at particular stamen developmental stages, and will provide a useful platform for dissecting the molecular mechanisms of developmental and reproductive biology in tomato and its wild relatives.

Conclusions

Based on distinct flower developmental stages, *S. pimpinellifolium* anther/stamen development was divided into ten stages and a correlation between the morphological characteristics and cytological landmark events at each developmental stage was established.

Acknowledgements

We would like to thank TGRC for providing us with *Solanum pimpinellifolium* (accession LA1585) seeds. We appreciate help from Dr. Jie Xu (School of Life Sciences and Biotechnology, Shanghai Jiao Tong University) with excellent semi-thin section work. We thank PlantScribe (www.plantscribe.com) for carefully editing this manuscript. The research was supported by grants from the Shanghai Science and Technology Committee (No.13391901202 and 14JC1403400), the China National '863' High-Tech Program (No.2011AA100607) and the National Natural Science Foundation of China (No. 31071810).

References

Alba, R., P. Payton, Z. Fei, R. McQuinn, P. Debbie, G.B. Martin, S.D. Tanksley and J.J. Giovannoni. 2005. Transcriptome and selected metabolite analyses reveal multiple points of ethylene control during tomato fruit development. *Plant Cell*, 17: 2954-2965.

Alvarez, A.E., C.C.M. Van de Wiel, M.J.M. Smulders and B. Vosman. 2001. Use of microsatellites to evaluate genetic diversity and species relationships in the genus *Lycopersicon*. *Theor. Appl. Genet.*, 103: 1283-1292.

Anonymous. 2012. The tomato genome sequence provides insights into fleshy fruit evolution. *Nature*, 485: 635-641. Please check not cited in the text

Barnabas, B., P.F. Fransz and J.H.N. Schel. 1987. Ultrastructural studies on pollen embryogenesis in maize (*Zea mays* L.). *Plant Cell Rep*., 6: 212-215.

Bedinger, P.A., R.T. Chetelat, B. McClure, L.C. Moyle, J.K.

Rose, S.M. Stack, E. van der Knaap, Y.S. Baek, G. Lopez-Casado, P.A. Covey, A. Kumar, W. Li, R. Nunez, F. Cruz-Garcia and S. Royer. 2011. Interspecific reproductive barriers in the tomato clade: opportunities to decipher mechanisms of reproductive isolation. *Sex. Plant Reprod.*, 24: 171-187.

Brukhin, V., M. Hernould, N. Gonzalez, C. Chevalier and A. Mouras. 2003. Flower development schedule in tomato *Lycopersicon esculentum* cv. sweet cherry. *Sex. Plant Reprod*., 15: 311-320.

Chang, F., Y.X.Wang, S.S.Wang and H. Ma. 2011. Molecular control of microsporogenesis in *Arabidopsis*. *Curr. Opin. Plant Biol*., 14: 66-73.

Chetelat, R.T. and V. Meglic. 2000. Molecular mapping of chromosome segments introgressed from *Solanum lycopersicoides* into cultivated tomato (*Lycopersicon esculentum*). *Theor. Appl. Genet.*, 100: 232-241.

Firdous, S., H. Ahmed, M. Hussain and M. Shah. 2015. Pollen morphology of *Ajuga* L., *Lamium* L. and *Phlomis* L. (Lamiaceae) from District Abbottabad Pakistan. *Pak. J. Bot.*, 47(1): 269-274.

Goldberg, R.B., T.P. Beals and P.M. Sanders. 1993. Anther development: basic principles and practical applications. *Plant Cell*, 5: 1217-1229.

Koltunow, A.M., J. Truettner, K.H. Cox, M. Wallroth and R.B. Goldberg. 1990. Different temporal and spatial gene expression patterns occur during anther development. *Plant Cell*, 2: 1201-1224.

Li, W. and R.T. Chetelat. 2010. A pollen factor linking inter- and intraspecific pollen rejection in tomato. *Science*, 330: 1827-1830.

Ma, H. 2005. Molecular genetic analyses of microsporogenesis and microgametogenesis in flowering plants. *Annu. Rev. Plant Biol*., 56: 393-434.

Marshall, J.A., S. Knapp, M.R. Davey, J.B. Power, E.C. Cocking, M.D. Bennett and A.V. Cox. 2001. Molecular systematics of *Solanum* section *Lycopersicum* (*Lycopersicon*) using the nuclear ITS rDNA region. *Theor. Appl. Genet.*, 103: 1216-1222.

Matas, A.J., T.H. Yeats, G.J. Buda, Y. Zheng, S. Chatterjee, T. Tohge, L. Ponnala, A. Adato, A. Aharoni, R. Stark, A.R. Fernie, Z. Fei, J.J. Giovannoni and J.K. Rose. 2011. Tissue and cell type specific transcriptome profiling of expanding tomato fruit provides insights into metabolic and regulatory specialization and cuticle formation. *Plant Cell*, 23: 3893-3910.

Mazzucato, A., A.R. Taddei and G.P. Soressi. 1998. The *parthenocarpic fruit* (*pat*) mutant of tomato (*Lycopersicon esculentum* Mill.) sets seedless fruits and has aberrant anther and ovule development. *Development*, 125:107-114.

Miller, J.C. and S.D. Tanksley. 1990. RFLP analysis of phylogenetic relationships and genetic variation in the genus *Lycopersicon*. *Theor. Appl. Genet.*, 80: 437-448.

Moyle, L.C. 2008. Ecological and evolutionary genomics in the wild tomatoes (*Solanum* sect. *Lycopersicon*). *Evolution*, 62: 2995-3013.

Mueller, L.A., T.H. Solow, N. Taylor, B. Skwarecki, R. Buels, J. Binns, C. Lin, M. H. Wright, R. Ahrens, Y. Wang, E. V. Herbst, E. R. Keyder, N. Menda, D. Zamir and S. D. Tanksley. 2005. The SOL Genomics Network. A comparative resource for Solanaceae biology and beyond. *Plant Physiol*., 138: 1310-1317.

Osorio, S., R. Alba, C.M. Damasceno, G. Lopez-Casado, M. Lohse, M.I. Zanor, T. Tohge, B. Usadel, J.K.C. Rose, Z. Fei, J.J. Giovannoni and A.R. Fernie. 2011. Systems biology of tomato fruit development: combined transcript, protein, and metabolite analysis of tomato transcription factor (*nor, rin*) and ethylene receptor (*Nr*) mutants reveals novel regulatory interactions. *Plant Physiol*., 157: 405-425.

Peralta, I.E., S. Knap and D.M. Spooner. 2006. Nomenclature for wild and cultivated tomatoes. *TGC Report*, 56: 6-12.

Polowick, P.L. and V.K. Sawhney. 1992. Ultrastructural changes in the cell wall, nucleus and cytoplasm of pollen mother cells during meiotic prophase in *Lycopersicorl esculenturn* Mill. *Protoplasma*, 169: 139-147.

Polowick, P.L. and V.K. Sawhney. 1993a. An ultrastructural study of pollen development in tomato (*Lycopersicon esculenturn*). I. Tetrad to early binucleate stage. *Can. J. Bot.*, 71: 1039-1047.

Polowick, P.L. and V.K. Sawhney. 1993b. An ultrastructural study of pollen development in tomato (*Lycopersicon esculentum*). II. Pollen maturation. *Can. J. Bot.*, 71: 1048-1055.

Polowick, P.L. and V.K. Sawhney. 1995. Ultrastructure of the tapetal cell wall in the stamenless-2 mutant of tomato (*Lycopersicon esculentum*): correlation between structure and male-sterility. *Protoplasma*, 189: 249-255.

Sanders, P.M., A.Q. Bui, K. Weterings, K.N. McIntire, Y.C. Hsu, P.Y. Lee, M.T. Truong, T.P. Beals and R.B. Goldberg. 1999. Anther developmental defects in *Arabidopsis thaliana* male-sterile mutants. *Sex. Plant Reprod*., 11: 297-322.

Sato *et al*., 2011. missing in ref. list.

Sawhney, V.K. and S.K. Bhadula. 1988. Micro-sporogenesis in the normal and male-sterile stamenless-2 mutant of tomato (*Lycopersicon esculentum*). *Can. J. Bot.*, 66: 2013-2021.

Sun, Y., Y. Wang, Y.Y. Li, J.Z. Jiang, N.N. Yang, C. Niu and Y. Li. 2015. Effects of colchicine treatment on the microtubule cytoskeleton and total protein during microsporogenesis in *Ginkgo biloba* L. *Pak. J. Bot.*, 47(1): 159-170.

Tanksley, S.D. 2004. The genetic, developmental, and molecular bases of fruit size and shape variation in tomato. *Plant Cell*, 16: S181-S189.

Yeats, T.H., K.J. Howe, A.J. Matas, G.J. Buda and T.W. Thannhauser. 2010. Mining the surface proteome of tomato (*Solanum lycopersicum*) fruit for proteins associated with cuticle biogenesis. *J. Exp. Bot.*, 61: 3759-3771.

Yousuf, Z., M.A. Khan and Z.K. Shinwari. 2009. A new variety of *Solanum surattense* Burm. from Pakistan. *Pak. J. Bot*., 41(6): 2097-2103.

Yousuf, Z., S. Masood, Z.K. Shinwari, M.A. Khan and M.A. Rabbani. 2006. Evaluation of taxonomic status of medicinal species of the genus solanum and capsicum based on poly acrylamide gel electrophoresis. *Pak. J. Bot*., 38(1): 99-106.

Zhang, D., X. Luo and L. Zhu. 2011. Cytological analysis and genetic control of rice anther development. *J. Genet. Genomics*, 38: 379-390.

Zhang, D.B. and Z.A. Wilson. 2009. Stamen specification and anther development in rice**.** *Chin. Sci. Bull.*, 54: 2342-2353.

Zuriaga, E., J. Blanca and F. Nuez. 2009. Classification and phylogenetic relationships in *Solanum* section *Lycopersicon* based on AFLP and two nuclear gene sequences. *Genet. Res.. Crop Evol.*, 56:663-678.

(Received for publication 2 May 2014)